2016 IEEE-RAS 16th International Conference on
Humanoid Robots (Humanoids)
Cancun, Mexico, Nov 15-17, 2016

Adaptation of Robot Physical Behaviour to Human Fatigue in Human-Robot Co-Manipulation

Luka Peternel, Nikos Tsagarakis, Darwin Caldwell and Arash Ajoudani

***Abstract*— In this paper, we propose a method that allows the robot to adapt its physical behaviour to the human fatigue in human-robot co-manipulation tasks. The robot initially imitates the human to perform the collaborative task in a leader-follower setting, using a feedback about the human motor behaviour. Simultaneously, the robot obtains the skill in online manner. When a predetermined level of human fatigue is detected, the robot uses the learnt skill to take over the physically demanding aspect of the task and contributes to a significant reduction of the human effort. The human, on the other hand, controls and supervises the high-level interaction behaviour and performs the aspects that require the contribution of both agents in such a dynamic co-manipulation setup. The robot adaptation system is based on the Dynamical Movement Primitives, Locally Weighted Regression and Adaptive Frequency Oscillators. The estimation of the human motor fatigue is carried out using a proposed online model, which is based on the human muscle activity measured by the electromyography. We demonstrate the proposed method with experiments on a real-world co-manipulation task with environmental constraints and dynamic uncertainties.**

I. Introduction

The high exploitation potential and fast growing demands of service robotics applications in home or industrial workspaces have led to the development of several well performing robots equipped with rich proprioception sensing and actuation control. Such systems that range from robotic manipulators [1] to full humanoids [2], [3] are expected to help the human user in various tasks, some of which require collaborative effort for successful and comfortable execution. A good example within this category is the cooperative tool use where the existence of dynamic uncertainties and environmental constraints call for an appropriate level of cognitive (high-level) and physical interaction between the robot and the human.

An essential part of any kind of human-robot collaboration is the ability of the robot to adapt its behaviour to the intention[1] and states of the human partner. This problem has been a central research focus in many human-robot collaboration studies, where various online interfaces have been developed. One of the most common types of the intention-recognition interfaces is based on the force sensing on the robot side [4]–[9]. Another common types of interfaces to determine the human intention are based on visual feedback [10] or auditory commands [11]. Alternatively, the intention can be read through human-induced motion during the execution of the task [12]. To achieve a more dynamic shared authority between the human and the robot, we recently proposed an interface [13] (based on tele-impedance principle [14]) where the intention of the cooperating human partner is read through the acquired muscle activity signals and his/her limb dynamic manipulability measure. As an alternative to direct intention recognition, the robot can use human demonstration [5], [12], [15], [16] or gradual adaptation [17] to derive the collaborative skill.

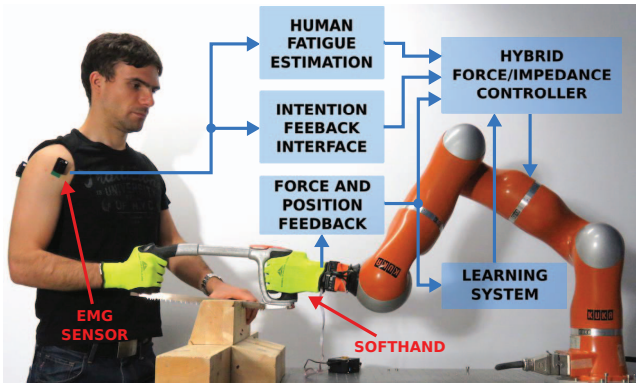

Fig. 1: The proposed human-robot co-manipulation framework for robot adaptation to human fatigue. The robot is controlled by a hybrid force/impedance controller. The myoelectric feedback interface provides the robot controller with a feedback about human motor behaviour to achieve an appropriate impedance profile in different phases of the task. The human fatigue estimation system provides the robot with the state of the human physical endurance. The learning system allows the robot to acquire skill of the task execution during the cooperation with the human partner and then replicate it when the human fatigue is detected.

What is common in most of the above human-robot cooperation scenarios is the assumption that the human partner has a constant level of physical endurance. This assumption can be considered to be true for simplistic tasks that require small physical effort or short execution time. However, other rough and more dynamic interaction scenarios can affect the human performance. While in [17] the human effort is minimised due to the nature of the method, the fatigue was not estimated or monitored. Indeed, unlike a sturdy humanoid robot, the human partner is prone to the physical fatigue; a subject-dependent phenomenon that can affect his/her physical interaction capabilities rapidly and unpredictably [18]. In such a case, the robot should be able to recognise the human fatigue and adapt its behaviour to offer additional physical support in the given task. As a result, the human partner should then only supervise the task on a cognitive level and produce less physical effort.

While the physical fatigue of the human is a well-studied

Authors are with HRI[2] Lab and HHCM Lab, Department of Advanced Robotics, Istituto Italiano di Tecnologia, Genoa, Italy, Email: luka.peternel@iit.it

This work was supported in part by the H2020 project CogIMon (ICT-23-2014, 644727).

[1]Intention is the current objective and task, not future state estimation.

subject in neuroscience and physiology [18]–[20], there are only a few studies of human fatigue in human-robot collaboration setting. In a recent study, Sadrfaridpour et al. [21] used a model-based human muscle fatigue estimation [20] to adjust the working speed of collaboration in a component assembly task. The task of the robot was to pick the necessary parts and place them near the human, who then sequentially performed the assembly alone. Nevertheless, this method did not address direct physical human-robot interaction or simultaneous co-manipulation (i.e. human and robot were not physically coupled with a tool/object while performing the task). In addition, robot behaviour did not change beyond adaptation of the execution speed.

In this paper, we examine the human fatigue in human-robot co-manipulation and propose a novel method that allows the robot to adapt and modulate the delivered physical assistance as a function of the human fatigue. Initially, using our proposed technique in [13], the robot establishes a hybrid controller and adapts its task impedance and trajectories to the human partner's behaviour. In this phase, the robot gradually learns the appropriate trajectories from the cooperation with the human using an online machine learning technique [12]. Once the human fatigue is detected online, the robot uses the learnt skill and offloads the human partner of the main physical stress. As a consequence, the human continues to supervise the operation and executes the aspects of the task that the robot cannot fully take over (i.e. cognitive and those which require collaborative effort).

The estimation of the human fatigue is based on a new model that is similar to the dynamical response of an RC circuit. This model has a similar dynamics to the previously proposed models based on the human muscle force [20]. The main difference is that our model estimates the fatigue based on the observed muscle activity obtained from the electromyography (EMG). One advantage of muscle activity based model is that it can also provide the information of effort that comes from muscle co-contraction, which cannot be observed through the measured force at the endpoint or measured torque in the joint. Another advantage is that force measurement is not required on the human side.

We demonstrate the proposed approach with experiments on KUKA Lightweight Robot equipped with a Pisa/IIT Softhand (see Fig. 1 for the setup). We selected a cooperative task of wood sawing using a two-person saw. This experimental task has been shown to provide challenging conditions for experimental analysis of human-robot co-manipulation [12], [13], and therefore should be suitable to validate the proposed method.

II. Methods

The proposed method is described by block scheme in Fig. 1. We controlled the motion of the robot by a hybrid force/impedance controller that uses information about the human intention provided by a muscle activity based human-robot interface [13]. We estimated fatigue of the collaborating human partner by a model that was based on the human muscular effort measured by EMG. The robot learned the physical behaviour (reference motion trajectories) during the initial stages of collaborative task execution. We used Dynamical Movement Primitives (DMPs) [22] to encode the robot motion trajectories, which were learnt online by Locally Weighted Regression [23]. The robot used Adaptive Frequency Oscillators [24] to estimate the desired task execution speed and control the phase and frequency of the learnt DMPs.

A. Robot Control Based on Human Intention Feedback

A hybrid force/impedance controller was implemented to govern the robot motion and force behaviour and was defined as

$$\boldsymbol{F}_{int} = \boldsymbol{F}_{force} + \boldsymbol{K}\big(\boldsymbol{x}_d - \boldsymbol{x}_a\big) + \boldsymbol{D}\big(\dot{\boldsymbol{x}}_d - \dot{\boldsymbol{x}}_a\big), \tag{1}$$

where $\boldsymbol{F}_{int}$ is the Cartesian space interaction force/torque acting from the robot on the environment, $\boldsymbol{x}_a$ is actual and $\boldsymbol{x}_d$ is reference pose of the robot end-effector, and $\boldsymbol{K}$ and $\boldsymbol{D}$ are robot virtual stiffness and damping matrices in Cartesian space. The term $\boldsymbol{F}_{force}$ is related to the force task and performs force control in predefined axes (z-axis in our case). We used this term to maintain the contact between the tool and the environment. $\boldsymbol{F}_{force}$ was controlled by a PI controller based on the force feedback[2]. The proportional gain of PI force controller was set to 0.5 and integral gain to 1.0.

The robot controlled the stiffness in different phases of the collaborative task by a feedback based on the estimated human intention. In our experimental task (i.e. collaborative sawing) the robot had to produce reciprocal/inverse behaviour in each phase compared to the human counterpart. If the human pulled the saw, the robot had to command a low stiffness to comply with the motion. In the opposite case, when the saw reached the human's end, the robot had to became stiff to pull the saw back to the reference position at the robot's end. The Cartesian stiffness matrix was defined as [13]

$$\boldsymbol{K} = \boldsymbol{K}_{const} + \boldsymbol{S}_K\big(1 - k_r\big), \tag{2}$$

where $\boldsymbol{S}_K$ is a diagonal matrix that is used to select the axes in which the stiffness should be modulated (in our case sawing motion axis), $\boldsymbol{K}_{const}$ is matrix that is used to set constant stiffness for the other axes and k_r is robot stiffness modulation parameter defined as [13]

$$k_r = c'_h(k_{max} - k_{min}) + k_{min}, \tag{3}$$

where $c'_h = a \cdot c_h$ is scaled human-estimated stiffness index c_h from the intention interface ($c'_h \in [0,1]$ and $c_h \in [0,1]$) and k_{max} and k_{min} are maximum and minimum controllable robot stiffness range.

Estimation of human stiffness trend was defined as [25]

$$c_h = b_1 \frac{1 - e^{-b_2(A_1+A_2)}}{1 + e^{-b_2(A_1+A_2)}}, \tag{4}$$

where A_1 and A_2 are muscle activation levels of dominant muscles acting on the shoulder joint. The measurement of

[2]The force measurement can be noisy due to the rough interaction with the environment [12], [13]. Therefore, we did not use derivative term in the controller to avoid stability issues.

antagonistic muscles enables detection of both pulling and pushing actions. In this experiment we used posterior and anterior fibres of Deltoid muscle that actuate the human shoulder joint. Parameter b_1 defines the maximum amplitude of mapping and b_2 defines the shape of mapping. Parameter a determines the task-related operational range of mapping. Parameters $b_1 = 20$, $b_2 = 0.05$ and $a = 12$ were determined experimentally as in [13].

Muscle activity for each muscle was measured by EMG using Delsys Trigno Wireless system. We processed (filtered and rectified) and normalised the EMG signals using maximal voluntary contraction (MVC). The mapping between the processed EMG and muscle activation level was defined as

$$0 \leq A_i(t) = \frac{EMG_i(t)}{MVC_i} \leq 1, \tag{5}$$

where A_i is muscle activation level for each muscle i, $EMG(t)$ is processed EMG signal and MVC is EMG signal under maximal voluntary contraction.

B. Human Fatigue Estimation

We based our human fatigue model on RC circuit dynamics, which corresponds well to fatigue dynamics observed/modelled in human studies [20]. The capacitor voltage (normalised to the source voltage) is equivalent to fatigue, conductance of the resistor is equivalent to the current effort of the muscle and capacitance of the capacitor is equivalent to the capacity of the muscle in terms of endurance. We defined the muscle fatigue estimation model as

$$V_i(t) = 1 - e^{-\int \frac{G_i(t)}{C_i} dt}, \tag{6}$$

$$G_i(t) = A_i(t), \tag{7}$$

where $V_i \in [0 \;\; 1]$ represents the fatigue index, G_i is parameter that represents the current effort dynamics and C_i is fatigue-related capacity of the given muscle i. Parameter C encodes human muscle specifics and should be tuned based on the individual subject and muscles used in the given task. The higher the parameter C is, the more effort G over time it takes for the fatigue to take effect.

We estimated the parameter C for each muscle by a preliminary experiment. In this experiment, we instructed the human to produce a reference muscle activity A_{ref} by exerting muscle force until he/she could not endure it any more[3]. We measured the time T_{end} that the human could endure each reference effort G_{ref} (in our experiment we used two reference efforts: 0.2 and 0.5). We obtained the fatigue capacity C for each reference by using the subject-dependant endurance time T_{end} and an assumption that full capacity is reached at $V = 0.993$ (corresponding to five time constants)

$$C = -\frac{G_{ref} \cdot T_{end}}{\log(1 - 0.993)}. \tag{8}$$

The final parameter C for a specific muscle was obtained by an average value of C for each reference, and was equal to 4.57 s for anterior and 4.82 s for posterior Deltoid muscle. In this preliminary study we only considered charging of C. This model can be expanded to include discharging of C to model human recuperation when the effort is reduced.

In the proposed approach, the robot takes over the production of the specified task aspect when either of V_i reaches some predetermined threshold V_{th}. In our experiments, we set this threshold to $V_{th} = 0.7$ for both muscles, which corresponds to 70% of the estimated endurance capacity. This value was chosen to avoid excessive human fatigue and discomfort. At that point, the trajectory learning stopped and the robot repeated the learnt behaviour according to the estimated execution speed. The human partner could then partially relax and recover some of the physical strength, while he/she continued to perform the collaborative aspects that the robot cannot take over by itself. Examples include: stabilisation of the saw movements at the human end, high-level decisions such as pausing and resuming the task execution, and changing the task coordinates as described in [13].

C. Robot Adaptation

We used periodic DMPs to encode the robot behaviour that was learnt from the collaboration with the human. The DMP is based on the dynamics of second-order system [22]

$$\dot{z} = \Omega\left(\alpha\left(\beta\left(-y\right) - z\right) + f\right), \tag{9}$$

$$\dot{y} = \Omega z, \tag{10}$$

where y is the encoded trajectory, f is the term that modulates the trajectory shape, $\alpha = 8$ and $\beta = 2$ are positive constants and Ω is the execution frequency.

The desired motion trajectory shape f_d was approximated as in [26] by

$$f_d = \frac{\ddot{x}_d}{\Omega^2} - \alpha\left(\beta\left(-x_d\right) - \frac{\dot{x}_d}{\Omega}\right). \tag{11}$$

where x_d, $\dot{x}_d$ and $\ddot{x}_d$ are the robot motion that we wish to learn and its derivatives. The desired trajectory shape f_d was used to build a nonlinear shape function f in (9) defined as [22]

$$f(\phi) = \frac{\sum_{i=1}^{N} \psi_i(\phi) w_i}{\sum_{i=1}^{n} \psi_i(\phi)}, \tag{12}$$

where w are weights used to determine shape of trajectory and $\psi_i(\phi)$ are Gaussian kernels uniformly distributed across the phase space ϕ. Kernels were defined as

$$\psi_i(\phi) = e^{h(\cos(\phi - c_i) - 1)}. \tag{13}$$

where h determines the width, c_i centres and N number of Gaussian kernels. We selected $N = 25$ in our experiments.

Each weight w_i of kernel ψ_i was updated using recursive least squares method [23]

$$w_i(t+1) \quad = \quad w_i(t) + \psi_i P_i(t+1) r e_r(t), \tag{14}$$

$$e_r(t) = f_d(t) - w_i(t) r, \tag{15}$$

[3]Note that this fatigue estimation procedure is subject-dependant. The subject was asked to endure the effort until task production became uncomfortable due to the muscle fatigue.

$$P_i(t+1) = \frac{1}{\lambda}\left(P_i(t) - \frac{P_i(t)^2 r^2}{\frac{\lambda}{\psi_i} + P_i(t) r^2}\right), \qquad (16)$$

where λ is forgetting factor that controls the forgetting rate of older data and was set to 0.995 for our experiments. Initial setting of parameters was $r = 1$, $w_i(0) = 0$ and $P_i(0) = 1$ for $i = 1, 2, ..., N$.

Phase and frequency of the learnt DMP were controlled by an adaptive oscillator (see [24] for details on adaptive oscillators). The adaptive oscillator outputs the phase and frequency estimation of some input signal. Parameters of adaptive oscillator were set the same as in [17]. The estimation was done based on the actual robot motion x_a (input signal) that enabled the human to alter the execution speed during the compliant phase of the robot motion [12].

III. Experiments

The task of the human and the robot was to use a two-person crosscut saw to cooperatively cut a beam of wood at different locations. Relatively large saw teeth demanded the saw to be cooperatively held at both ends to stabilise it during the rough interaction with the environment. The robot end-effector motion and force were controlled by (1). The robot controlled the sawing motion (x-axis) indirectly through stiffness modulation based on the feedback from the human muscle activity interface (2). The controllable stiffness range of the robot in x-axis was set to $k_{max} = 1500$ N/m and $k_{min} = 75$ N/m. The initial reference position in x-axis was pre-programmed to the position at the robot's end where it should pull the saw. The y-axis was aligned in parallel with the beam of wood and its stiffness was set to a constant value of $k = 0$ N/m. This allowed the human to freely guide the robot and determine the incision location. The contact force between the saw and wood was maintained in z-axis by the PI controller. For this experiment we set the reference z-axis force to $F_d = -5$ N.

Please refer to supplementary multimedia file for a video of the experiment. The results of the experiment are shown in Fig. 2. The human partner initially guided the robot towards the desired incision location on the beam and inserted the saw blade inside the hole. When the contact with the material was established, the two cooperating partners started to produce the task (see top-left photo). The human began to increase the muscle activity (see first graph) to pull the saw whenever the blade ended at the robot's end (see fourth graph, red line). The robot recognised the intention of the human and became compliant when the human was pulling the saw in order not to obstruct the effort (see third graph). When the saw position reached the human's end and the human stopped pulling, the robot started to increase the stiffness to bring the saw back to its own end. Reciprocally, the human remained compliant while the robot was pulling in order not to obstruct the robot effort. This procedure then periodically repeated where the human was given an approximate reference frequency of execution $\Omega = 1.0$ Hz.

At the beginning of the sawing task the robot started to estimate the human physical fatigue based on the proposed model (6). See the second graph of Fig. 2 for this estimation. While the task was cooperatively executed with the human partner, the robot used machine-learning module to learn the motion trajectory. The human fatigue gradually increased until it reached the predetermined level of 70% endurance capacity. Note that in this preliminary study we did not include recuperation model, therefore C did not discharge and V remained at 70%. At that point the robot used the learnt behaviour and took over the part of task execution that involved driving the blade across the beam (i.e. x-axis motion). The moment of this switch is marked by a black vertical line in the second graph. The robot then increased the stiffness and started to reproduce the learnt reference trajectory (see fourth graph). The task reproduction was done at a frequency that was estimated in the previous stage (see fifth graph).

After the robot took over the x-axis motion aspect of the task the human muscle activity could significantly reduce (see first graph). The human could then recuperate some of his/her strength, while maintaining the aspects of the cooperative task that robot cannot take over. One of such important aspects is stabilisation of the saw at the human side.

The human also remained in control of supervision and cognitive aspects of the task. We demonstrated this by instructing the human to make the sawing at a different location along the beam. The human first used a voice command to instruct the robot to temporary halt the task production. This point is indicated by a purple vertical line in the second graph. At that point the robot halted the reference x-axis motion trajectory at that phase. The human then lifted the saw outside of the current hole and moved it into a different hole (see top-middle photo).

When the saw was re-inserted into a new hole and the contact with the material was established the voice command was used again to instruct the robot to continue to produce the task using the learnt behaviour. This point is indicated by a green line in the second graph. The robot then resumed the cooperation and the task was produced (see top-right photo). However, the human had to remain present to stabilise the saw during the cutting. This was especially crucial in the initial stages as the hole was not as deep and therefore the saw easily could move out (see also supplementary video). Therefore, such tasks still require human presence and collaborative effort, despite the robot obtaining the skill and taking over a major task aspect.

We performed additional experiments to examine the response of the system at different cooperation speed. We instructed the human to produce the task with higher ($\Omega =$ 1.25 Hz) and lower frequency ($\Omega = 0.5$ Hz). The results are shown in Fig. 3. The left column graphs are related to the lower execution frequency, while the right column graphs are related to the higher execution frequency. The execution with the lower frequency took less effort from the human as lower friction and inertial forces were required in order to drive the saw. This can be observed by comparing the muscle activity in both cases (see first row graphs). The robot therefore took

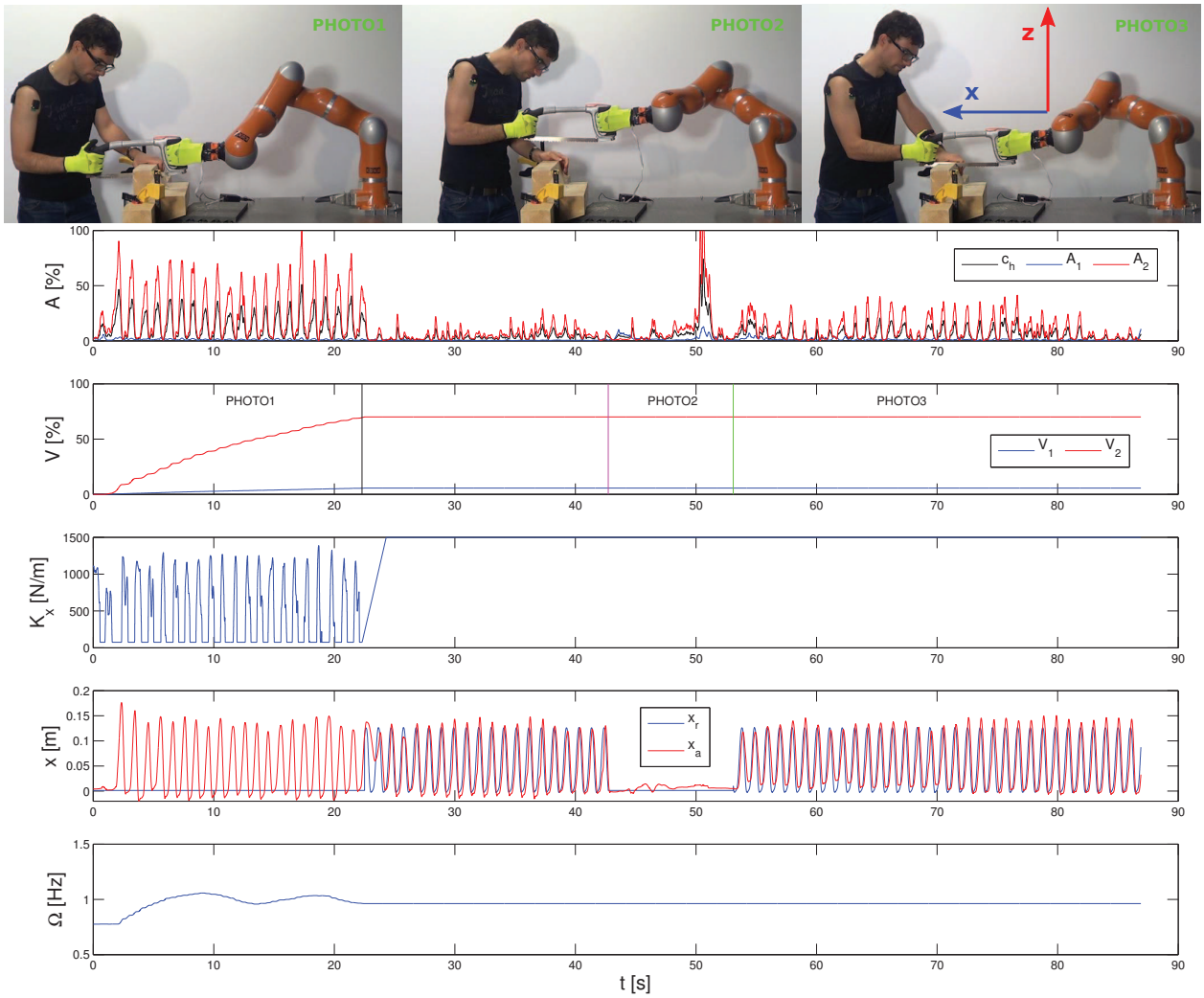

Fig. 2: Results of the main experiment. The photos at the top were taken during the experiment and correspond to different stages of the task. The stage to which each photo corresponds to is indicated by the text in the second graph. The first graph shows the human muscle activity related measurements (A_1 is anterior and A_2 is posterior Deltoid). The second graph shows the estimated fatigue for each muscle. The third graph shows the robot end-effector stiffness in the sawing motion axis (x-axis). The fourth graph shows reference (blue) and actual (red) robot end-effector motion in the sawing axis. The fifth graph shows the task execution frequency as estimated by an adaptive oscillator.

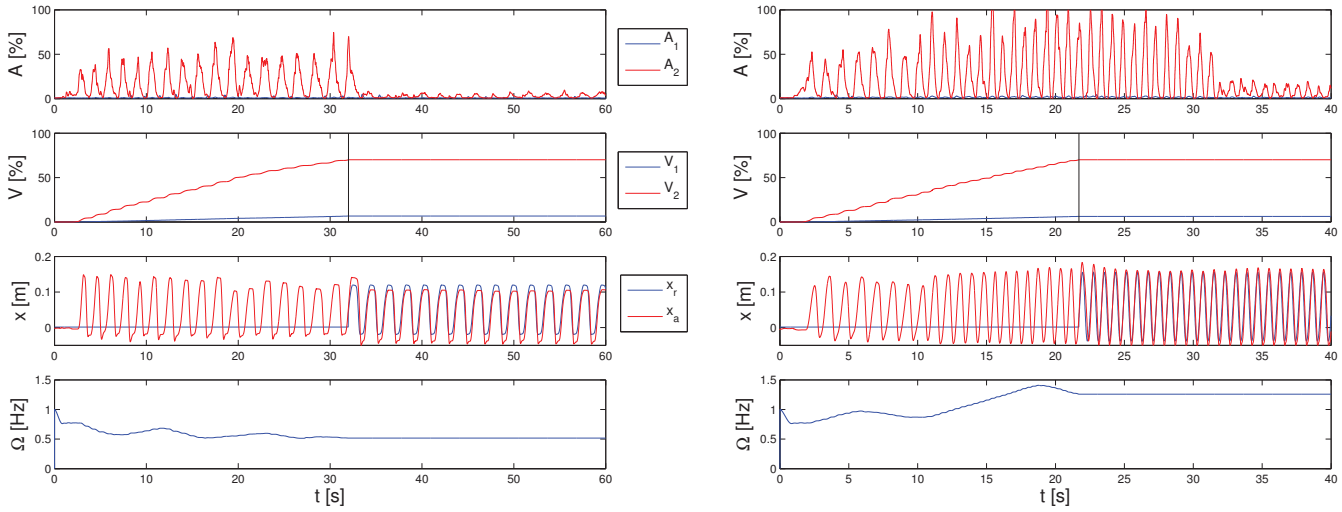

Fig. 3: Results of additional experiments. The left column graphs show the experiment where the task was produced with lower frequency (reference $\Omega = 0.5$ Hz). The right column graphs show the experiment where the task was produced with higher frequency (reference $\Omega = 1.25$ Hz).

over the sawing motion at a later time compared to the higher execution frequency (see second row graphs). For the lower execution frequency, the fatigue threshold was reached after 32.0 s. For the higher execution frequency, the threshold was reached at 21.7 s.

From the first graph in the right column we can see that the human can still choose to be involved and assist the blade motion even after the robot takes over the lead. The human can then stop producing that aspect of the task arbitrary based on the preference or because of the constraint due to the physical fatigue.

IV. Discussion

To give the robot an estimation of the human muscle fatigue level, we proposed a new fatigue model based the measured human EMG signals. Currently, the proposed human fatigue estimation model only predicts the endurance. In future we will extend it to include human recuperation. When the human muscles are relaxed, the fatigue-related capacitor in (6) should gradually discharge to model the recuperation.

Initially, we tried using the median frequency of power density spectrum of measured EMG signal to estimate the human muscle fatigue. It has been shown that the median frequency of power density spectrum decreases and its amplitude increases as a result of muscle fatigue [18]. While this kind of estimation was good in case of constant muscle contraction as observed in [18], in our task the observed estimation was unpredictable and inconsistent. This can probably be attributed to rapid changes in muscle activation amplitude that are required due to the dynamic nature of the selected co-manipulation task. Such changes probably affected the dynamics of observed median frequency. In addition, in such case it is difficult to determine the appropriate sampling window to track the median frequency changes throughout the task execution.

The existing proof-of-concept study was limited to a single subject. In future we will perform multi-subject analysis to acquire more insights about the application of the proposed method. Additionally, other collaborative human-robot tasks will be considered.

References

[1] A. AlbuSchäffer, S. Haddadin, C. Ott, A. Stemmer, T. Wimböck, and G. Hirzinger, "The DLR lightweight robot: design and control concepts for robots in human environments," *Industrial Robot: An Intl. Journal*, vol. 34, no. 5, pp. 376–385, 2007.

[2] N. Tsagarakis, D. G. Caldwell, A. Bicchi, F. Negrello, M. Garabini, L. B. W. Choi, V. Loc, J. Noorden, M. Catalano, M. Ferrati, L. Muratore, A. Margan, L. Natale, E. Mingo, H. Dallali, A. Settimi, A. Rocchi, V. Varricchio, L. Pallottino, C. Pavan, A. Ajoudani, J. Lee, P. Kryczka, and D. Kanoulas, "WALK-MAN: A high performance humanoid platform for realistic environments," *Journal of Field Robotics*, p. Accepted, 2016.

[3] K. Kaneko, K. Harada, F. Kanehiro, G. Miyamori, and K. Akachi, "Humanoid robot HRP-3," in *Intelligent Robots and Systems (IROS), 2008 IEEE/RSJ Intl. Conf. on*, Sept 2008, pp. 2471–2478.

[4] K. Kosuge and N. Kazamura, "Control of a robot handling an object in cooperation with a human," in *Robot and Human Communication, 6th IEEE Intl. Workshop on*, Sep 1997, pp. 142–147.

[5] P. Evrard, E. Gribovskaya, S. Calinon, A. Billard, and A. Kheddar, "Teaching physical collaborative tasks: object-lifting case study with a humanoid," in *IEEE-RAS Intl. Conf. on Humanoid Robots*, 2009, pp. 399–404.

[6] E. Gribovskaya, A. Kheddar, and A. Billard, "Motion learning and adaptive impedance for robot control during physical interaction with humans," in *Robotics and Automation (ICRA), 2011 IEEE Intl. Conf. on*, May 2011, pp. 4326–4332.

[7] S. Ikemoto, H. Ben Amor, T. Minato, B. Jung, and H. Ishiguro, "Physical human-robot interaction: Mutual learning and adaptation," *Robotics Automation Magazine, IEEE*, vol. 19, no. 4, pp. 24 –35, Dec 2012.

[8] P. Donner and M. Buss, "Cooperative swinging of complex pendulum-like objects: Experimental evaluation," *IEEE Transactions on Robotics*, vol. 32, no. 3, pp. 744–753, June 2016.

[9] L. Peternel and J. Babič, "Learning of compliant human-robot interaction using full-body haptic interface," *Advanced Robotics*, vol. 27, no. 13, pp. 1003–1012, Jun 2013.

[10] D. Agravante, A. Cherubini, A. Bussy, P. Gergondet, and A. Kheddar, "Collaborative human-humanoid carrying using vision and haptic sensing," in *Robotics and Automation (ICRA), 2014 IEEE Intl. Conf. on*, May 2014, pp. 607–612.

[11] J. Medina, M. Shelley, D. Lee, W. Takano, and S. Hirche, "Towards interactive physical robotic assistance: Parameterizing motion primitives through natural language," in *RO-MAN, 2012 IEEE*, Sept 2012, pp. 1097–1102.

[12] L. Peternel, T. Petrič, E. Oztop, and J. Babič, "Teaching robots to cooperate with humans in dynamic manipulation tasks based on multi-modal human-in-the-loop approach," *Autonomous robots*, vol. 36, no. 1-2, pp. 123–136, Jan 2014.

[13] L. Peternel, N. Tsagarakis, and A. Ajoudani, "Towards multi-modal intention interfaces for human-robot co-manipulation," in *Intelligent Robots and Systems (IROS), 2016 IEEE/RSJ Intl. Conf. on*, October 2016.

[14] A. Ajoudani, N. G. Tsagarakis, and A. Bicchi, "Tele-impedance: Teleoperation with impedance regulation using a body-machine interface," *I. J. Robotic Res.*, vol. 31, no. 13, pp. 1642–1656, 2012.

[15] L. Rozo, D. Bruno, S. Calinon, and D. G. Caldwell, "Learning optimal controllers in human-robot cooperative transportation tasks with position and force constraints," in *Intelligent Robots and Systems (IROS), 2015 IEEE/RSJ Intl. Conf. on*, 2015.

[16] M. Ewerton, G. Neumann, R. Lioutikov, H. B. Amor, J. Peters, and G. Maeda, "Learning multiple collaborative tasks with a mixture of interaction primitives," in *Robotics and Automation (ICRA), 2015 IEEE Intl. Conf. on*, May 2015, pp. 1535–1542.

[17] L. Peternel, T. Noda, T. Petrič, A. Ude, J. Morimoto, and J. Babič, "Adaptive control of exoskeleton robots for periodic assistive behaviours based on EMG feedback minimisation," *PLoS ONE*, vol. 11, no. 2, p. e0148942, Feb 2016.

[18] C. J. De Luca, "Myoelectrical manifestations of localized muscular fatigue in humans." *Critical reviews in biomedical engineering*, vol. 11, no. 4, pp. 251–279, 1984.

[19] R. M. Enoka and J. Duchateau, "Muscle fatigue: what, why and how it influences muscle function," *The Journal of physiology*, vol. 586, no. 1, pp. 11–23, 2008.

[20] L. Ma, D. Chablat, F. Bennis, and W. Zhang, "A new simple dynamic muscle fatigue model and its validation," *Intl. Journal of Industrial Ergonomics*, vol. 39, no. 1, pp. 211 – 220, 2009.

[21] B. Sadrfaridpour, H. Saeidi, J. Burke, K. Madathil, and Y. Wang, *Modeling and Control of Trust in Human-Robot Collaborative Manufacturing*. Boston, MA: Springer US, 2016, pp. 115–141.

[22] A. J. Ijspeert, J. Nakanishi, and S. Schaal, "Learning rhythmic movements by demonstration using nonlinear oscillators," in *Intelligent Robots and Systems (IROS), 2002 IEEE/RSJ Intl. Conf. on*, 2002, pp. 958–963.

[23] S. Schaal and C. G. Atkeson, "Constructive incremental learning from only local information," *Neural Comput.*, vol. 10, no. 8, pp. 2047–2084, Nov. 1998.

[24] T. Petrič, A. Gams, A. J. Ijspeert, and L. Žlajpah, "On-line frequency adaptation and movement imitation for rhythmic robotic tasks," *Int. J. Rob. Res.*, vol. 30, no. 14, pp. 1775–1788, Dec. 2011.

[25] A. Ajoudani, S. Godfrey, M. Bianchi, M. Catalano, G. Grioli, N. Tsagarakis, and A. Bicchi, "Exploring teleimpedance and tactile feedback for intuitive control of the pisa/iit softhand," *Haptics, IEEE Transactions on*, vol. 7, no. 2, pp. 203–215, April 2014.

[26] A. Gams, A. Ijspeert, S. Schaal, and J. Lenarčič, "On-line learning and modulation of periodic movements with nonlinear dynamical systems," *Autonomous robots*, vol. 27, no. 1, pp. 3–23, 2009.